Metabolomics (2009) 5:59–71
DOI 10.1007/s11306-008-0139-x

ORIGINAL ARTICLE

A metabolomics approach to assessing phytotoxic effects on the green alga *Scenedesmus vacuolatus*

Christina Kluender · Frédéric Sans-Piché · Janet Riedl · Rolf Altenburger · Claus Härtig · Grit Laue · Mechthild Schmitt-Jansen

Received: 20 June 2008 / Accepted: 28 October 2008 / Published online: 22 November 2008

Abstract The potential of metabolomics for toxicity analysis with synchronized algal populations during growth was explored in a proof of principle study. Low molecular weight compounds from hydrophilic and lipophilic extracts of algal populations of the unicellular green alga *Scenedesmus vacuolatus* were analyzed using gas chromatography-mass spectrometry (GC-MS) and subsequent multivariate analysis to identify time-related patterns. Algal metabolite responses were studied under control and exposure conditions for the photosystem II-inhibiting herbicide prometryn. To define the typical metabolic profile of control *S. vacuolatus* cultures seven time points over a growth period of 14 h were evaluated. The results show a clear time-related trend in metabolite levels and a distinct separation of exposed and reference algal populations. The results suggest an impairment of the energy metabolism associated with an activation of catabolic processes and a retardation of carbohydrate biosynthesis in treated algae. Metabolite results were compared to observation parameters, currently used in phytotoxicity assessment, showing that metabolites respond faster to exposure than algal growth. The potential of metabolomics for toxicity evaluation, especially to identify physiological markers and to detect effects at an early state of exposure, are discussed. Therefore, we suggest a metabolomics approach utilizing synchronous algal cultures to be a suitable future tool in ecotoxicology.

Keywords Synchronous algal growth · Ecotoxicology · Phenotypic anchoring · Environmental risk assessment · Mixture toxicity · Periphyton · Metabolic profiling · Triazine

1 Introduction

The assessment of risks of chemicals towards biota in aquatic systems is one of the major concerns of environmental research. Chemicals may directly or indirectly affect all relevant ecosystem functions like primary production, where the macro- and microalgae constitute the basic organisms of this fundamental ecosystem function. Toxicity evaluation of chemicals mainly relies on non-specific population-based observation parameters, such as the inhibition of growth or reproduction. Current ecotoxicology is faced with challenges, such as the extrapolation of chronic effects from acute observations (Raimondo et al. 2007) or signalling potential damage in the environment by early warning systems, like biomarkers (Hansen 2008). Additionally, challenges from combined effects from mixture exposure in the environment or mode-of-action analysis of new chemicals (Escher and Hermens 2002) or understanding of differences in species sensitivity towards toxicants (Altenburger and Schmitt-Jansen 2003) are acknowledged. None of these issues can be dealt using growth-based approaches solely, but improvements may be achieved from metabolomics (Ankley et al. 2006).

C. Kluender · F. Sans-Piché · J. Riedl · R. Altenburger · M. Schmitt-Jansen (✉)
UFZ—Helmholtz Centre for Environmental Research, Bioanalytical Ecotoxicology, Permoserstrasse 15, 04318 Leipzig, Germany
e-mail: Mechthild.Schmitt@ufz.de

C. Härtig
UFZ—Helmholtz Centre for Environmental Research, Environmental Microbiology, Permoserstrasse 15, 04318 Leipzig, Germany

G. Laue
Novartis Institutes for BioMedical Research, WSJ-360.6.02, 4056 Basel, Switzerland

Metabolomics aims at the identification and quantification of all the metabolites present in a biological sample at an unbiased level (Dettmer et al. 2007). During growth, a dynamic response of the biochemical network of a cell manifests in alterations of the metabolic pattern. Therefore, insights in the underlying biochemical processes, involved in the interaction of a chemical with an organism, may significantly contribute to understanding of toxic actions. Metabolomics has successfully been applied in environmental studies (e.g. Lin et al. 2006; Hines et al. 2007) and in stress physiology for studying nutrient depletion in algae (Bölling and Fiehn 2005), freezing tolerance of plants (Cook et al. 2004) or temperature stress (Guy et al. 2008). Metabolomics was developed for aquatic toxicity analysis with molluscs and fish (Viant et al. 2002, 2005, 2006a, b; Samuelsson et al. 2006; Turner et al. 2007; Ekman et al. 2007) and in terrestrial ecotoxicology to earthworms (Bundy et al. 2004; Jones et al. 2008) and *Arabidopsis thaliana* cell cultures (Le Lay et al. 2006; Sarry et al. 2006; Ducruix et al. 2008). In aquatic phytotoxicity assessment, a metabolomics based approach has not been proposed to our knowledge.

One challenge in ecotoxicology is to provide information at an early state of exposure in the sense of subacute toxic effects, even before they may become manifest in common toxicological observation parameters of the phenotype. Knowledge on time-related metabolic responses of an organism to a xenobiotic could contribute to a mechanistic understanding of effects and thus foster mode-of-action analysis of toxicants. Light-induced synchronous cultures of microalgae are ideally suited to investigate cell cycle related metabolic events and its perturbations (Krupinska and Humbeck 1994). In synchronous algal cultures, all individuals of the population are in the same developmental stage and will reproduce within the same period of time. Intra-specific variation at a given developmental stage is considered to be minimal in these clonal populations of genetically identical algae. It is therefore possible to define developmental metabolic trajectories (Viant et al. 2005) of these cultures. Synchronized cultures of the unicellular freshwater chlorophyte *Scenedesmus vacuolatus* are successfully used to assess toxic effects on one generation cycle of this alga (Altenburger et al. 2004). Chlorophytes are relevant test organisms in phytotoxicity assessment for regulatory purposes, such as OECD guideline 201 (2006) or ISO 8692 (2002). Moreover, fundamental ecotoxicological research is performed with the chlorophyte *S. vacuolatus*, e.g. studies on mixture toxicity concepts (Altenburger et al. 2004) or mode-of-action-analysis (Adler et al. 2007; Altenburger et al. 2006; Franz et al. 2008) or effect-directed identification of phytotoxicants in environmental samples (Brack et al. 1999). Therefore, this test organism provides a good linkage to currently used observation parameters in ecotoxicology.

The aim of this study was to establish a combined approach for phytotoxicity evaluation by linking biochemical responses of the microalga *S. vacuolatus* after exposure to growth responses. In a proof of principle study first, the experimental variability of the approach was characterised by analysing several samples in parallel. In a second experiment, the variation of the metabolic pattern of a synchronous culture of the chlorophyte was characterised during a growth period of 14 h. Subsequently, deviations from this pattern during toxic exposure were studied. To be able to link chemical-induced changes in the metabolite profile to understanding mechanisms of toxicity, a model compound with a well-known mode-of-action, the photosystem (PS) II-inhibiting herbicide prometryn, was chosen. An experimental design was developed for multi-parallel analysis of low-molecular weight hydrophilic and lipophilic algal compounds by using gas chromatography-mass spectrometry and multivariate pattern recognition.

2 Materials and methods

2.1 Algal cell culture

The unicellular freshwater chlorophyte (*Scenedesmus vacuolatus* Shih. et Krauss strain 211-15) was acquired from the culture collection Pringsheim (SAG Göttingen, Germany). Populations were grown in sterile medium (pH 6.4) as given in Faust et al. (1992). During a 24 h cell cycle, algae were cultured under synchronous conditions, as described by Faust et al. (2001) and Altenburger et al. (2004). Thus, *S. vacuolatus* was sustained by cultivating the alga each day in fresh medium inoculated with 10^6 cells per ml from a previously grown *S. vacuolatus* population. The following culture parameters were used: illumination with saturated white light at an intensity of approximately 400 µmol photons s^{-1} m^{-2} in a 14:10-h light:dark cycle, bubbling regime with compressed air and 1.5% CO_2, and 28°C medium temperature. Furthermore, cultural synchronisation was monitored daily according to Altenburger et al. (2004). Parameters of algal growth and cell density were determined using an electronic cell analyser (CASY®1, Schärfe System GmbH; Reutlingen, Germany). The parameters: algal cell number, cell diameter in µm and cell volume in fl (femto litre) (1 fl = 10^{-9} µl) were measured during 14 h of algal growth and quantified by applying a protocol presented by Altenburger et al. (2008).

Two sets of experiments were performed to assess the variation of the metabolic pattern of a synchronous culture. First, the experimental variability of the approach was characterised by the parallel analysis of several cultures of

S. vacuolatus, grown for 14 h (Experiment I). In a second experiment, changes of the metabolite pattern were studied in control and exposed algal cultures over the growth period of 14 h (Experiment II).

2.2 Experiment I: statistical analysis of experimental variability

Experimental variability of quantity data was evaluated in three sets of experiments: (i) Variation deriving from the synchronous culture was analysed with four independent replicates of algal populations, 14 h grown in different cylinders. (ii) Variation deriving from the metabolomics protocol applied in this study was estimated with four samples from the same algal population, 14 h grown in one cylinder. (iii) The technical error of the GC-MS system was determined using a data set from a 4-fold analysis of the calibration standard mixture of a homologous series of 24 *n*-alkanes (C8–C32) (Sigma Technical Bulletin; Saint Louis, USA). This standard mixture has been additionally analysed every fifth run within a sequence of algal extracts. The mean coefficients of experimental variance (CV) were calculated for each peak area of selected signals and averaged over all signals.

2.3 Experiment II: toxicity evaluation

The phytotoxicity assay started with a homogenous population of *Scenedesmus vacuolatus* cells at the beginning of the cell cycle (in the following named t_0-cells). Exposure experiments were performed with an initial density of 10^6 algal cells ml^{-1} in sterilised glass cylinders. Cylinders were filled with a total volume of 300–600 ml in dependence to the harvested algal biomass (see section 'Harvest'). Cells were exposed to 0.1 µmol l^{-1} prometryn (stock solution 0.103 mmol l^{-1} in DMSO). About 99.7% pure prometryn (2-methylthio-4.6-bisisopropyl-amino-1.3.5-triazine, CAS RN 7287-19-6) was available from Riedel-de-Häen (Seelze, Germany). The prometryn concentration of 0.1 µmol l^{-1} was chosen according to pre-studies, showing a 65% inhibition of algal reproduction after 24 h of exposure. The chosen prometryn concentration ensured well defined effects on growth inhibition, especially after short incubation times, but also reversible, non-lethal effects in terms of retardation of the cell cycle (Adler et al. 2007). From the starting culture of *S. vacuolatus*, two entire cylinders were harvested (t_0-cells, $N = 2$). From growth stage 0 h on, controls were incubated with 0.1% DMSO and treatments were incubated with prometryn in 0.1% DMSO. At six further time-points, the entire cultural material from one cylinder was harvested to derive sufficient algal material for further sample preparation. Thus after 4, 6, 8, 10, 12 and 14 h of algal incubation (in the following named t_4, t_6, t_8, t_{10}, t_{12} and t_{14}-cells, respectively), one control and two independent replicates of prometryn-treated algae were harvested.

2.4 Harvest

The size of *Scenedesmus vacuolatus* cells differed remarkably in the range from 20 to 200 fl in the bioassays, due to algal growth and growth inhibition by prometryn. In order to obtain similar algal biomass from each sample, a total of 10 µl fresh biomass was harvested. Therefore, the final culture volume, which was used for harvesting, was adapted to the cell size of *S. vacuolatus*. Cells with at least 3 µm mean diameter were filtered with Isopore membrane filters (polycarbonate, 0.4 µm pore size) (Millipore S.A.S.; Molsheim, France) in a vacuum driven AS 310/3 three-place filtration system (Schleicher & Schuell GmbH – Whatman Group; Dassel, Germany). During filtering, algal cells were washed twice with 20 mM NaCl, which corresponds to the salts concentration in the standard cultural medium. In the above described status, the algal cells have been shown to be fully active from previous NMR-studies (Altenburger et al. 1995). Additionally, membrane integrity was surveyed by staining cells with propidiumiodid and subsequent measurements with flow-cytometry according to Adler et al. (2007). These measurements revealed no changes in membrane integrity during the harvest process (data not shown). The biomass was washed with 20 mM NaCl from the filter into an 80 ml tube and centrifuged at 3,300*g* for 5 min at 22°C. The resulting pellet was transferred into a 2 ml tube and the supernatant was discarded. After further centrifugation at 4,000*g* for 10 min at 22°C, the supernatant was removed and the remaining pellet with algal cells was quick-frozen in liquid nitrogen. Afterwards, samples were lyophilized and stored at −70°C for less than 7 days until cell disruption.

In addition, procedure blanks were prepared to detect contaminations of the alga metabolome deriving from the metabolomics procedure up to the sample analysis by GC-MS. The blanks were prepared by filtering the cultural media as harvested for algal reference samples. In the following procedure blanks were treated the same as algal samples.

2.5 Metabolite extraction

Algae cells were disintegrated using the cell disruptor Genie (Milian; Meyrin, Switzerland). One ml of a 4°C cold single-phase solvent mixture of methanol, chloroform and 0.015% trifluoroacetic acid in water (10:5:4, v/v/v)

was added. Methanol and chloroform were purchased from Merck (Darmstadt, Germany) in the highest purity grade available. Trifluoroacetic acid (99.5%) was purchased from Fluka (Buchs, Switzerland). Also 150 mg of glass beads with a diameter of 0.5 mm (Carl Roth GmbH; Karlsruhe, Germany) were added to each sample. Glass beads were washed in sulphuric acid and distilled water before use and metabolite extraction was carried out at 5°C for 15 min in the dark. The suspension was centrifuged for 5 min at 20,000*g* at 5°C, and 0.9 ml of the supernatant were decanted into a 10 ml glass tube. The pellet was discarded.

In order to separate hydrophilic and lipophilic metabolites, a liquid–liquid extraction was performed. Phases of different polarity were obtained by adding 0.8 ml of bi-distilled water and 1.6 ml of chloroform, intensive shaking of the mixture for 20 s and centrifugation for 10 min at 5,000*g* at 5°C. In total, three phases were separated. From the upper hydrophilic methanol/water phase and from the lower lipophilic chloroform/methanol phase, 0.9 ml extract were transferred into 3 ml reaction glass vials. The remaining middle phase was discarded. All samples were dried under a stream of nitrogen at 40°C for a maximum of 3 h.

2.6 Derivatisation

Metabolites from hydrophilic and lipophilic extracts were derivatised in two steps and analysed by GC-MS using protocols modified after Roessner et al. (2000) and Fiehn et al. (2000). The derivatisation protocol was modified regarding the incubation temperature of samples in the derivatisation reagent. This enabled the parallel processing of hydrophilic and lipophilic fractions, which was saving time. Also, the temperature program of the GC-MS analysis protocol was modified to enhance separation of hydrophilic and lipophilic compounds of *Scenedesmus vacuolatus* extracts in the chromatogram.

The first step of the derivatisation of hydrophilic compounds was the methoximation to prevent ring formation and to stabilise carbonyl moieties (Roessner et al. 2000). Reduced hydrophilic residues were incubated with 200 µl of 2% methoxyamine HCl in pyridine (MOX) for 120 min at 80°C. MOX was acquired from Pierce (Rockford, USA). In parallel, dried samples from the lipophilic metabolite fraction were esterified with 300 µl methanolic HCl for 240 min at 80°C. Methanolic HCl (hydrochloric acid in methanol) was purchased from Supelco (Bellefonte, USA). The hydrophilic and lipophilic fractions were dried under a stream of nitrogen at 40°C and for 20 min silylated in 100 µl of *N*-methyl-*N*-(trimethylsilyl) trifluoroacetamide (MSTFA) at 90°C. MSTFA was acquired from Pierce (Rockford, USA).

2.7 GC-MS measurement

Derivatised samples of hydrophilic and lipophilic *Scenedesmus vacuolatus* metabolites were analysed with a gas chromatography-mass spectrometry (GC-MS) system. All system components originated from Agilent Technologies (Santa Clara, USA) including the 6890 N gas chromatograph coupled to a quadrupole 5975 mass spectrometric detector. The system was equipped with electron impact ionisation (EI), an autosampler (7683 series) and an injector (7683B series). The machine was controlled by the instrument's ChemStation software (G1712DA, Rev. 02.00).

One µl of the sample was injected (split ratio of 3:1, carrier gas helium) into a deactivated pre-column (10 m), which was connected to a middle polar DB 35-ms column (30 m length, 0.25 mm internal diameter, 0.25 µm film) (Agilent Technologies; Santa Clara, USA). Injection and interface temperature were 280°C, the quadrupole was set to 150°C and the ion source was adjusted to 230°C. The separation of hydrophilic metabolites was achieved with an oven temperature program of 1 min isothermal at 100°C, followed by a 5°C min^{-1} temperature ramp to 260°C, followed by 20°C min^{-1} temperature ramp to 350°C and a final 5 min heating at 350°C. To stabilize retention times from run to run, the retention time locking software (RTL) (Agilent Technologies; Santa Clara, USA) was used. The head pressure was adjusted in the constant pressure mode to the locked retention time 17.380 min (17.5 psi) of the reference compound octadecane. Mass spectra were recorded after a solvent delay of 4 min with 2.46 scans per second (mass scanning range of *m*/*z* 50–650; threshold abundance value of 50). Lipophilic samples were analysed by GC-MS using the same parameters as described for the hydrophilic phase, with the exception that the injection split ratio was set to 20:1 and the head pressure was adjusted to a locked retention time of 29.700 min (17.2 psi) for the new reference compound eicosane. Moreover, the temperature program was modified: the initial oven temperature was set to 60°C (1 min isocratic) followed by a temperature ramping with 5°C min^{-1} to 320°C and a final 3 min heating at 320°C. For RTL, head pressure was adjusted to retention time of eicosane at 29.7 min and set at constant mode.

Within the GC-MS sequence of algal extracts a calibration standard mixture of a homologous series of 24 *n*-alkanes (C8–C32) (Sigma Technical Bulletin; Saint Louis, USA) has been analysed every fifth run for the determination of retention time indices.

2.8 Data preprocessing

The assignment of metabolites was processed using the Automated Mass Spectral Deconvolution and Identification

System (AMDIS, software vs. 2.62). Within the AMDIS analysis, spectra of detected compounds were searched against custom spectrum library from the National Institutes of Standards and Technology (NIST 2005) and were assigned based on the retention index. Applying the minimum spectrum similarity match factor (correspondence of the found mass spectra with the library spectra) of 70%, a rough insight into the metabolite composition of the chromatogram was gained. In addition, the mass spectral match factor of 90% was applied to gain biochemically more reliable assignments for the metabolite composition.

To enable quantitative data analysis, peak areas of non-deconvoluted chromatograms were integrated using the instrument's ChemStation software (Agilent, G1712DA, Rev. 02.00). Manual alignment was carried out on the basis of apical retention times and mass spectra similarity matches. Peak area data were manually aligned in the order of retention times. Chromatograms from algal samples were compared to reference chromatograms from procedure and solvent blanks. Peak areas from blank signals overlaying peaks from algae in an amount of more than 50% were excluded from further data analyses.

2.9 Multivariate data analysis

To determine changes or differences between the total ion currents or chromatograms (TIC) of various algal samples, principal component analysis (PCA) was performed using JMP IN 5.1 software (SAS; Cary, USA). PCA was used to reduce the dimensionality of the chromatographic data but to capture most of the variance. For the time course experiment, the reduced dataset after data-preprocessing was used for PCA. Data were mean centred and auto-scaled but not further transformed before PCA analysis.

3 Results

3.1 Toxicity assessment during algal growth

In order to link time-related patterns in the algal metabolome to adverse effects observed during growth inhibition, algal cultures were studied during a growth period of 14 h in the presence of prometryn (Fig. 1). After a lag-phase of 4 h, the cell volume of controls increased exponentially up to 10-fold within 14 h of growth. Cell volumes of exposed cells were consistently lower than those of reference algal populations. After 14 h of exposure, the median cell volume was about 86% smaller than that of control populations and the algae remained with their cell size in the range of t_4 cells of controls.

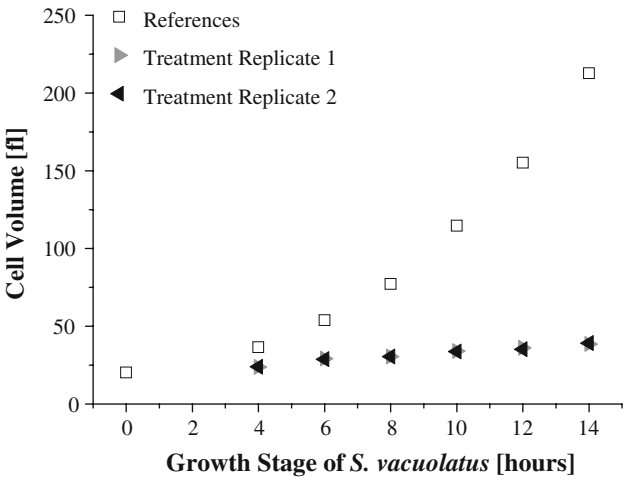

Fig. 1 Cell volume of synchronised cultures of *Scenedesmus vacuolatus* over time from 0 to 14 h of algal growth of references (□) and two replicates of treatment with 0.1 µmol l^{-1} prometryn ((▶) treatment replicate 1, (◀) treatment replicate 2). One data point represents the mean cell volume in femto-litre (fl) of one algal population. The mean was estimated throughout a cell counter system by measuring two replicates ($N = 2$) of an aliquot of one sample of the algal population, containing $\sim 2*10^5$ algal cells ml^{-1}. The system did not provide values of standard deviation for the mean of the cell volume

3.2 GC-MS data analysis

All algal samples gave reproducible characteristic chromatograms. A typical chromatogram of hydrophilic extracts from t_{14} control algae is shown in Fig. 2. Note that the *y*-axis is scaled linear and logarithmic before and after the break, respectively. By using AMDIS, 560 (t_0-cells) and 600 (t_{14}-cells) hydrophilic components as well as 210 (t_0-cells) and 340 (t_{14}-cells) lipophilic components were detected. Sugars, amino acids, organic acids, phosphoric compounds, glycerol and fatty acids were assigned and the hydrophilic assignments are summarized in Table 1. During data-preprocessing data were integrated based on non-deconvoluted chromatograms and corrected for procedure and solvent blanks, reducing the dataset substantially. Finally, 113 hydrophilic and 170 lipophilic compounds were selected for further statistical analysis.

After data-preprocessing the coefficients of variation (CVs) were calculated with the peak area values from samples from experiment (I) to assess experimental precision. The median of CVs from four independently analysed samples, which can represent the biological variation, averaged at 15%, and 95% of the data varied less than 50%. CVs for the technical scatter were determined with 4% and for the sample preparation with 20%. Comparable results were found for the lipophilic phase (data not shown). The biological variation seems to be relatively low in comparison to the variation derived from the procedure, which

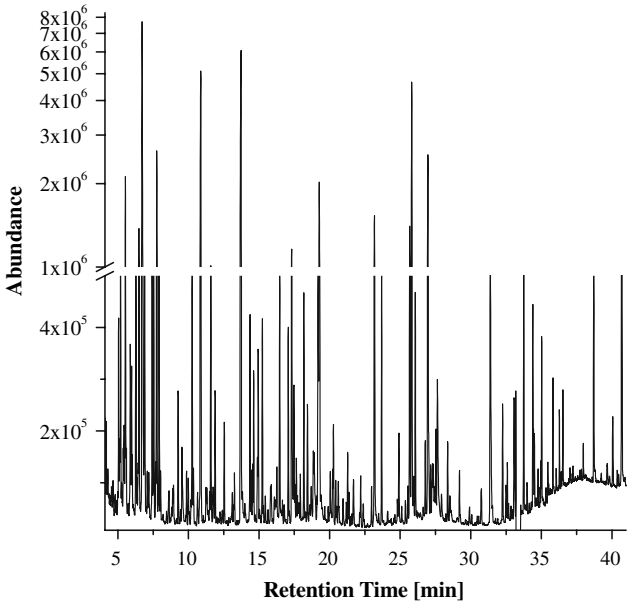

Fig. 2 A typical total ion current or chromatogram of hydrophilic fractions from 14 h old *Scenedesmus vacuolatus* cells. More than 500 compounds were found after deconvolution using AMDIS. Note change of the abundance scale from linear to logarithmic scale, after the break

clearly indicates the advantages of working with synchronous algal cultures.

3.3 Analysis of time-related metabolite patterns of reference algal populations

In hydrophilic and lipophilic metabolite extracts of untreated algal populations clear developmental changes during growth became evident due to a trend of scores from negative to positive values of PC 1 (Fig. 3). Score values, ranging from −4.5 (t_0-cells) to 15.3 (t_{14}-cells) increased continuously over time. The only exception was the sample taken after 12 h. Reference sample 12 showed normal growth characteristics (Fig. 1) but decreased concentrations in selected metabolites (e.g. sugars, Fig. 5d–f), indicating a failure in the analytical procedure. Therefore, this sample could be regarded as an outlier.

The observed pattern in the PCA score plot (Fig. 3) corresponds to the response ratios of several metabolites: In total, 29 hydrophilic and 10 lipophilic substances could be identified with a match accuracy of mass spectra of ≥90%. Studying the corresponding PCA loading plot (Fig. 4), sugars were identified as main drivers of sample separation during growth. They increased in controls but mainly remained at low levels in treated samples. 10 sugars could be identified from the hydrophilic fraction. Multivariate statistics revealed that 6 sugars were the main drivers of variation during the 14 h light phase (Fig. 4; Table 1). Glucose, which has been shown to be the dominant sugar in several *Chlorella* species (Brown and Jeffrey 1992), could not be identified with a match-accuracy higher than 86% and was therefore excluded from further analysis. Except of levoglucosane, all cellular concentrations of sugars increased during growth, with fructose showing the largest gain compared to t_0-cells (17-fold, Table 1) indicating accumulation of assimilation products from the Calvin cycle.

Thirteen amino acids were assigned showing varying dynamics during growth under control conditions (Table 1, additionally Gln and ornithine were identified). Except for Met, cellular concentrations of all amino acids increased during growth with Lys and Gly showing maximal gain (14.4-fold for Lys and 5.4-fold for Gly compared to t_0-cells, Table 1). For most of the amino acids the biggest relative increase was found after 8–10 h of growth indicating the dominance of anabolic processes in this phase. Time-related patterns of selected amino acids were not grouped according to biosynthetic families, with Val, Leu, Asp, Met, Phe and Tyr showing a maximum after 12 h but decreased towards the end of the light phase; cellular concentrations of Gly, Pro, Thr, Ala and Lys increased until the end of the light phase.

3.4 Metabolomics assessment of prometryn exposure

The PCA score plots (Fig. 3) indicated a clear separation of control and exposed algal populations by the first and second principal components, which together explained 45% of variability in the hydrophilic phase and 69% in the lipophilic phase. The consideration of further principal components did not improve the explanation of variability or the time-related trend in a better way.

Separation of exposed algal populations from controls became evident in the principal component 2 (PC2) after 4 h of exposure. The hydrophilic components (Fig. 3a) showed a time-related trend in PC2 until 12 h of exposure with increasing distance to controls. Parallel samples showed good accordance with exception of t_{10}-exposed cells. However, after 14 h of exposure the biochemical pattern of exposed algae (t_{14}-cells) seemed to correspond with initial cell stages of control algal populations. The time-related trend of the lipophilic phase showed comparable overall characteristics, but was less evident.

The PCA loading plot of 113 hydrophilic compounds in Fig. 4 corresponds to the PCA score plot in Fig. 3a. Several metabolites could be identified contributing to the sample separation. From the 113 hydrophilic metabolites, 51 metabolites were selected showing largest absolute loadings and are highlighted in Fig. 4. Twenty-nine of these 51 metabolites could be identified by data-base comparison with a match of ≥90% (Table 1). Identified

Table 1 Changes of the peak area values of 29 identified hydrophilic metabolites from *Scenedesmus vacuolatus* regarding time (growth from 0 to 14 hours) and prometryn treatment (0.1 µmol L^{-1}) (for further description see footnote)

Column 1	Column 2	Column 3						Column 4						Column 5					
Metabolites	Peak areas at growth stage t_0 ($N = 2$) ($\times 10^5$)	Metabolite time–response ratio: references at a specific growth stage ($c_{[tx]}$) compared with autospores ($c_{[t0]}$)						Metabolite time–response ratio: treatments (0.1 µmol l^{-1} prometryn) at a specific growth stage ($t_{[tx]}$) compared with autospores ($c_{[t0]}$)						Metabolite treatment-response ratio: treatments (0.1 µmol l^{-1} prometryn) at a specific growth stage ($t_{[tx]}$) compared with references at the same growth stage ($c_{[tx]}$)					
		$c_{[t4]}/c_{[t0]}$	$c_{[t6]}/c_{[t0]}$	$c_{[t8]}/c_{[t0]}$	$c_{[t10]}/c_{[t0]}$	$c_{[t12]}/c_{[t0]}$	$c_{[t14]}/c_{[t0]}$	$t_{[t4]}/c_{[t0]}$	$t_{[t6]}/c_{[t0]}$	$t_{[t8]}/c_{[t0]}$	$t_{[t10]}/c_{[t0]}$	$t_{[t12]}/c_{[t0]}$	$t_{[t14]}/c_{[t0]}$	$t_{[t4]}/c_{[t4]}$	$t_{[t6]}/c_{[t6]}$	$t_{[t8]}/c_{[t8]}$	$t_{[t10]}/c_{[t10]}$	$t_{[t12]}/c_{[t12]}$	$t_{[t14]}/c_{[t14]}$
Valine	50	1.0	1.0	2.0	2.0	2.0	2.0	1.0	1.0	1.0	1.0	2.0	1.0	1.0	1.0	1.0	1.0	1.0	1.0
Glycerol	167	2.0	2.0	2.0	2.0	2.0	3.0	1.0	1.0	1.0	1.0	1.0	1.0	1.0	0.4	0.5	0.5	1.0	0.5
Leucine	65	1.0	2.0	2.0	2.0	2.0	2.0	1.0	1.0	2.0	1.0	2.0	1.0	1.0	1.0	1.0	1.0	1.0	1.0
Glycine*	58	2.0	2.0	3.0	4.0	5.0	5.0	2.0	2.0	2.0	3.0	3.0	3.0	2.0	1.0	1.0	1.0	1.0	0.5
Proline	55	2.0	2.0	2.0	2.0	3.0	4.0	1.0	1.0	1.0	2.0	2.0	1.0	1.0	1.0	0.5	1.0	1.0	0.3
Butanedioic acid1	376	1.0	1.0	1.0	1.0	1.0	2.0	1.0	1.0	1.0	1.0	1.0	1.0	1.0	1.0	1.0	1.0	1.0	1.0
Threonine	78	2.0	2.0	2.0	2.0	2.0	2.0	2.0	2.0	2.0	2.0	2.0	2.0	1.0	1.0	1.0	1.0	1.0	1.0
Alanine	9	1.0	1.0	1.0	1.0	1.0	2.0	2.0	1.0	1.0	1.0	2.0	1.0	2.0	1.0	1.0	1.0	1.0	0.5
Butanedioic acid2	609	2.0	2.0	1.0	2.0	2.0	2.0	1.0	1.0	1.0	1.0	2.0	2.0	1.0	1.0	1.0	0.5	1.0	1.0
Aspartic acid*	127	4.0	2.0	2.0	4.0	4.0	2.0	12.0	14.0	15.0	13.0	12.0	5.0	3.0	8.0	7.0	4.0	3.0	3.0
Methionine	13	1.0	1.0	0.0	0.5	1.0	1.0	1.0	1.0	1.0	1.0	2.0	1.0	1.0	1.0	–	2.0	3.0	1.4
Pyrrolidone carboxylic acid	760	2.0	3.0	3.0	4.0	3.0	3.0	1.0	1.0	1.0	1.0	2.0	2.0	1.0	0.4	0.4	0.3	1.0	1.0
Butanediamine	19	1.0	2.0	2.0	2.0	1.0	2.0	1.0	0.0	0.0	0.0	0.3	0.5	1.0	0.0	0.0	0.0	0.2	0.3
Pentanedioic acid	19	2.0	3.0	4.0	0.0	3.0	4.0	0.3	0.2	1.0	0.3	1.0	1.0	0.2	0.1	0.1	–	0.3	0.3
Phenylalanine	30	1.0	1.0	1.0	1.0	2.0	1.0	1.0	2.0	2.0	2.0	3.0	2.0	1.0	1.0	2.0	1.0	2.0	1.0
Levoglucosan	30	1.0	1.0	1.0	1.0	1.0	1.0	0.2	0.0	0.2	0.0	0.4	1.0	0.2	0.0	0.3	0.0	0.5	1.0
Phosphoric compound 1	12	3.0	6.0	6.0	9.0	9.0	11.0	2.0	1.0	1.0	1.0	4.0	4.0	0.5	0.2	0.2	0.1	0.4	0.4
Phosphoric compound 2	39	3.0	4.0	5.0	6.0	6.0	8.0	2.0	1.0	2.0	1.0	4.0	4.0	1.0	0.3	0.3	0.2	1.0	0.4
Galactose	15	1.0	1.0	1.0	1.0	1.0	2.0	0.0	0.0	0.0	0.2	1.0	1.0	0.0	0.0	0.0	0.2	1.0	1.0
Fructose*	2	4.0	12.0	11.0	14.0	4.0	17.0	0.0	3.0	0.0	0.0	4.0	2.0	0.0	0.2	0.0	0.0	1.0	0.1
Mannose*	18	0.5	3.0	3.0	3.0	1.0	4.0	1.0	1.0	1.0	1.0	1.0	1.0	1.0	0.3	0.3	0.4	1.0	0.3
Propanoic acid	80	1.0	2.0	2.0	4.0	1.0	2.0	1.0	1.0	1.0	2.0	4.0	3.0	1.0	1.0	1.0	0.4	3.0	2.0
Lysine*	48	1.0	2.0	2.0	2.0	7.0	14.0	1.0	1.0	1.0	2.0	4.0	6.0	1.0	1.0	1.0	1.0	1.0	0.4
Tyrosine	24	2.0	2.0	2.0	2.0	2.0	2.0	1.0	1.0	2.0	2.0	3.0	2.0	1.0	1.0	1.0	1.0	1.0	1.0
Phosphoric compound 3	21	11.0	11.0	9.0	12.0	13.0	17.0	2.0	1.0	1.0	2.0	5.0	5.0	0.1	0.1	0.1	0.2	0.4	0.3
Oleic acid	38	1.0	1.0	1.0	1.0	1.0	1.0	1.0	1.0	1.0	1.0	1.0	1.0	1.0	1.0	1.0	1.0	1.0	1.0

Table 1 continued

Column 1	Column 2	Column 3				Column 4				Column 5			
Metabolites	Peak areas at growth stage t_0 ($N = 2$) ($\times 10^5$)	Metabolite time–response ratio: references at a specific growth stage ($c_{[tx]}$) compared with autospores ($c_{[t0]}$)				Metabolite time–response ratio: treatments (0.1 µmol l^{-1} prometryn) at a specific growth stage ($t_{[tx]}$) compared with autospores ($c_{[t0]}$)				Metabolite treatment-response ratio: treatments (0.1 µmol l^{-1} prometryn) at a specific growth stage ($t_{[tx]}$) compared with references at the same growth stage ($c_{[tx]}$)			
		$c_{[t4]}/c_{[t0]}$	$c_{[t6]}/c_{[t0]}$	$c_{[t8]}/c_{[t0]}$	$c_{[t10]}/c_{[t0]}$	$c_{[t12]}/c_{[t0]}$	$c_{[t14]}/c_{[t0]}$	$t_{[t4]}/c_{[t0]}$	$t_{[t6]}/c_{[t0]}$	$t_{[t8]}/c_{[t0]}$	$t_{[t10]}/c_{[t0]}$	$t_{[t12]}/c_{[t0]}$	$t_{[t14]}/c_{[t0]}$	$t_{[t4]}/c_{[t4]}$	$t_{[t6]}/c_{[t6]}$	$t_{[t8]}/c_{[t8]}$	$t_{[t10]}/c_{[t10]}$	$t_{[t12]}/c_{[t12]}$	$t_{[t14]}/c_{[t14]}$
Linolenic acid	10	2.0	2.0	2.0	3.0	3.0	4.0	1.0	1.0	2.0	1.0	3.0	3.0	1.0	0.5	1.0	0.3	1.0	1.0
Mannose-6-phosphate*	88	1.0	2.0	2.0	2.0	2.0	2.0	0.0	0.0	0.0	0.0	0.4	1.0	0.0	0.0	0.0	0.0	0.3	1.0
Glucopyranoside	22	0.0	4.0	6.0	3.0	2.0	11.0	0.0	0.0	0.0	1.0	1.0	0.0	1.0	0.0	0.0	0.3	0.3	0.0

These 29 metabolites (column 1) were identified via NIST-library with a spectral match quality ≥90% and were selected regarding their vector length by using principal component analysis (PCA), as shown in Fig. 3a. Column 2 shows the peak area values ($\times 10^5$) for t_0-cells, representative for the start of algal growth. The metabolite time–response ratios of references and treatments are shown for the developmental stages t_4, t_6, t_8, t_{10}, t_{12} and t_{14}. In column 3, the time–response ratio of metabolites from reference algae at a specific growth stage ($c_{[tx]}$) in comparison with the peak area of t_0-cells ($c_{[t0]}$) is given. Column 4 shows the time-response ratio of metabolites from treatment algae (mean of two independent replicates, $N = 2$) at a specific growth stage ($t_{[tx]}$) in comparison with the peak area of t_0-cells ($c_{[t0]}$, $N = 2$). In column 5, the response ratio of metabolites from treatment algae (mean of two independent replicates, $N = 2$) at a specific growth stage ($t_{[tx]}$), compared with reference algae ($N = 1$) at the same growth stage ($c_{[tx]}$), is shown. Peak area dynamics of metabolites labeled with asterisks (e.g. Glycine*), are exemplarily shown in Fig. 5

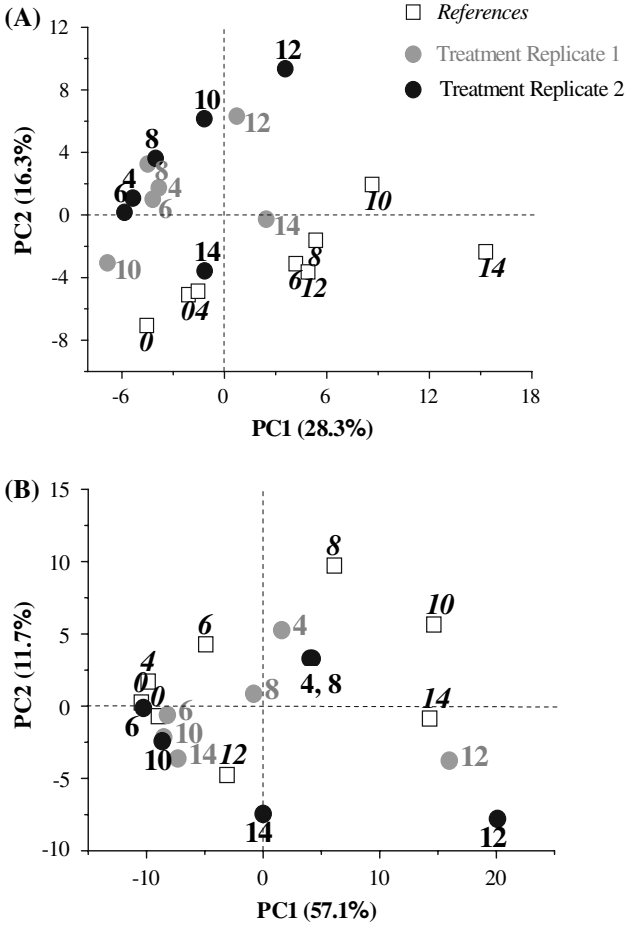

Fig. 3 Principal component analysis (PCA) score plots of first and second principal components (PCs) from **a** 113 hydrophilic and **b** 170 lipophilic compounds from *Scenedesmus vacuolatus* during growth from 0 to 14 h. The value of one PC (in %) explains a certain percentage of the total variability of the underlying data set. The PCA scores from references (□) as well as from two treatment-replicates (● and ●), exposed to 0.1 µmol l^{-1} prometryn are shown. Labels of sample scores indicate the growth stage of the microalgae in hours (e.g. $0 = t_0$). At stage t_0, two reference samples are shown to demonstrate variability between early stage replicates. For all other investigated algal growth stages at t_4, t_6, t_8, t_{10}, t_{12} and t_{14}, one control and two treatment replicates are shown

amino acids and sugars are labelled in Fig. 4. Sugars, such as mannose, fructose or galactose, received high absolute loadings on the axis of principal component 1 (PC1) and therefore contributed mainly to the separation of PCA scores of untreated algal populations during growth. Amino acids, such as Phe, Asp or Met, obtained high absolute loadings on the axis of PC2, indicating exposure-related changes in metabolites.

In summary, it became evident that axis PC1 mainly explains variability over time whereas axis PC2 was related to variability induced by the toxicant. Quantities and trends of selected metabolites over time are shown in Table 1 and Fig. 5. Three different time-exposure-related patterns could

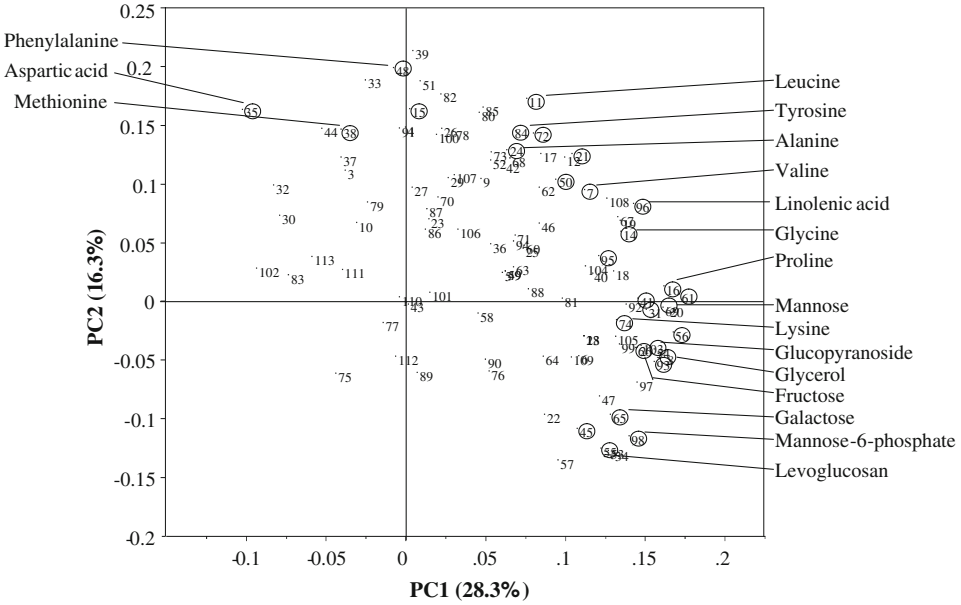

Fig. 4 PCA loading plot pattern of 113 hydrophilic compounds from *Scenedesmus vacuolatus* references and prometryn treatments (0.1 µmol l^{-1}) during growth from 0 to 14 h, described by the principal components 1 and 2. Numbers stand for the order of signals regarding their retention time in the GC-MS total ion chromatogram. Fifty-five compounds were found to be most important for the PCA score plot pattern, shown in Fig. 3a. Twenty-nine of these 55 compounds were assigned a chemical structure (via NIST-library with a spectral match quality ≥90%) and highlighted. Labels of loadings indicate assigned sugars and amino acids. Related response ratios of metabolite concentration levels are shown in Table 1

be characterised: (i) 'early exposure-specific increase in metabolites': In comparison to controls, Asp showed large changes after 4 h of exposure, already (12-fold in comparison to t_0-cells) and increased up to eight-fold in exposed cells in comparison to controls at a given time point, but decreased after longer exposure times (14 h) to control level (Table 1, Fig. 5a). (ii) 'late-observable effects': The amino acids Lys and Gly remained at low concentrations in both, exposed and control populations at initial growth but increased in control populations after 10–12 h of growth (Table 1; Fig. 5b and c). (iii) 'early exposure-specific inhibition of biosynthesis': The sugars increased immediately after growth in controls but remained at low concentrations in growth retarded algal populations (Fig. 5d–e) or were even consumed during the first 4 hours compared to controls at t_0 (Fig. 5f).

4 Discussion

The goal of this study was to determine if the strategy of a joint analysis of algal growth inhibition and pattern analysis of hydrophilic and lipophilic algal metabolites gives new insights in phytotoxicity assessment. To provide a first unbiased assessment of effects on the metabolic level after exposure, the GC-MS-based analysis of algal extracts was combined with multivariate data analysis. Subsequently, main drivers for PCA sample separation were identified by using a PCA loading plot. Time-related trends of these highly responsive metabolites were studied by time–response relationships.

To study stress-induced effects in organisms, the knowledge of the variability of the standard metabolic pattern of reference material is essential. To assess experimental precision, median relative coefficients of variation (CVs) of signal intensities from four samples (experiment I) were determined for the technical scatter (4%), for sample preparation (20%) and for the biological variation (15%), respectively. Fiehn et al. (2000) and Weckwerth et al. (2004) estimated mean relative CVs of about 8% for signals from the *Arabidopsis thaliana* wild type deriving from derivatisation, but 40% from 18 extracts from individually grown plants. They concluded that biological variation is the largest source of variability in the metabolomics approach. Broeckling et al. (2005) studied the metabolome of cell cultures from the legume *Medicago truncatula* and found CVs for the biological scatter in the range of 27–33%. In the present study, biological variation calculated from extracts from four samples was much lower indicating that metabolite extracts, derived from $>10^7$ genetically identical individuals from synchronized populations of the unicellular chlorophyte *S. vacuolatus*, reduced biological variation substantially. This clearly indicates the suitability of working with clonal populations in metabolomics. Individual level investigations introduce higher variability in metabolic profiles as described

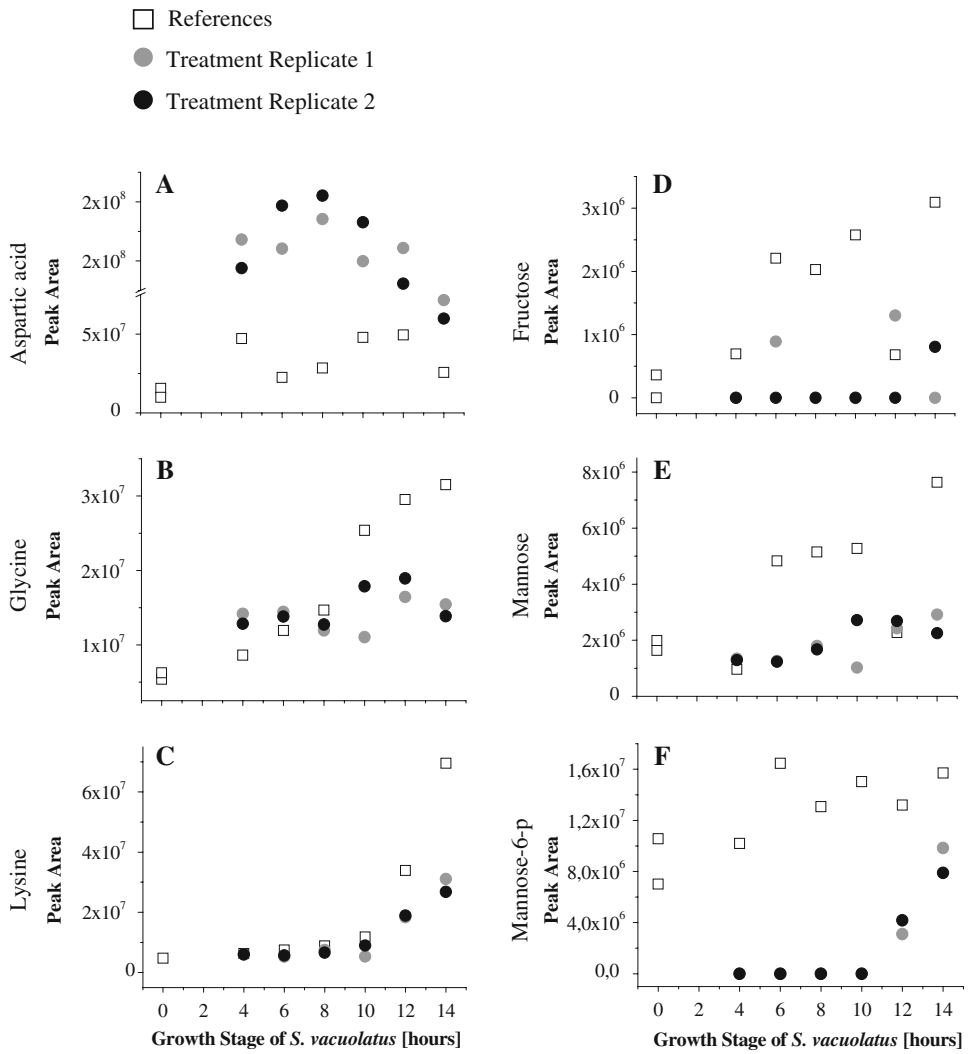

Fig. 5 Time dependent dynamics of the chromatographic peak area from six hydrophilic metabolites (aspartic acid, lysine, glycine, fructose, mannose and mannose-6-phosphate). These six metabolites were found to be important variables within the pattern of the PCA loading plot (Fig. 4). For each investigated algal growth stage in hours (t_4, t_6, t_8, t_{10}, t_{12} and t_{14}), one reference (□) and two treatment replicates (0.1 µmol l^{-1} prometryn) (● and ●) from *Scenedesmus vacuolatus* are shown. At stage t_0, two reference samples are shown to demonstrate variability between early stage replicates

recently in a metabolomics study on individual fish exposed in the laboratory (Ekman et al. 2007) and for mussels taken from the field (Hines et al. 2007).

Further improvements of the approach could be achieved by minimizing the variation deriving from sample preparation and by further quantifying the scatter of replications during growth. From the time-trends of selected metabolites, it got obvious that the concentrations of the compounds of the two replicates of exposed samples were nearly identical in the beginning of the growth phase but increasingly deviated after a longer growth period (Fig. 5b–f). This may indicate a manifestation of slightly different initial conditions of the cultures over time.

Viant (2007) introduced the concept of the normal metabolic operating range (NMOR) of an organism for metabolomics studies. As the metabolites are changing during the development of an organism, the NMOR has to be defined over time. In this proof of principle study, a first characterisation of the metabolic pattern of the primary metabolism of synchronized cultures of *S. vacuolatus* over a period of 14 h was done by applying a metabolomics approach: The estimated growth phase covers the postmitosis cell-cycle phase (G1) and a first S/M phase (DNA-synthesis and mitosis) (Krupinska and Humbeck 1994), which is characterised by an exponential increase of chlorophyll *a* and cell volume between 3 and 9 h after onset of the light phase. An increase of the algal cell volume up to 10-fold after 14 h of growth was found in this study (Fig. 1). After 7 h of growth, the cells are capable for mitosis, but it is the achieved cell volume at the end of the

growth phase determining the number of daughter cells, deriving from multiple fission (Vitovà and Zachleder 2005).

The increasing PC1-score values (Fig. 3) show a clear trend of defined developmental stages of reference cultures from *S. vacuolatus* indicating significant metabolic changes during growth. Sugars belong to the main drivers for sample separation during growth (high loading values in PC1, Fig. 4), indicating that produced sugars are not completely used for maintenance and cell growth but were accumulated and increased the available pool of assimilation products.

The amino acid patterns found in this study are in accordance with former studies: Kanazawa (1964) shows that the formation of free amino acids is in most parts light dependent. Moebus-Faust (1994) studied patterns of free amino acids of *S. vacuolatus* during growth using rp-HPLC for targeted analysis. She describes an immediate increase of the total amino acid-pool (per cell volume) within the first 4 h of growth but a decrease already 10 h after the onset of light. However, the dynamics of selected amino acids show varying patterns over time, which is also found in this study. A time-related relationship of biosynthesis of amino acids may be concluded from the dynamics of Asp and Lys. While Lys is increasing in both, reference and exposed algal populations at the end of the growth phase, Asp, which is the biochemical precursor of lysine, is decreasing at the end of the growth phase. Furthermore, Asp is involved in the biosynthesis of pyrimidines. The synchronous cultures enter the first S-phase (synthesis of DNA) after 10 h of growth, thus enhanced biosynthesis of pyrimidines and increased consumption of Asp may be assumed, which is consistent with a decrease of the Asp-pool after 12 h of growth.

In summary, the applied metabolomics approach revealed first insights into changes of the metabolite composition of *S. vacuolatus* during the light phase of the cell cycle. It therefore provides the basis for subsequent analysis of stress-induced changes after toxic exposure.

On a phenotypic level, the exposure of algal populations to prometryn caused an 86% inhibition of cell growth. Earlier studies, using several staining methods and flow cytometry for algal status acquisition, showed that algal cells are still vital after 14 h of exposure at the concentration used in this study but growth retarded (Adler et al. 2007). So we conclude that the shift in metabolite abundance observed here reflects a regulated compensatory response rather than a chaotic chain of events eventually leading to death of the organisms.

Exposed algal populations showed reliable separation of the cell stages t_4–t_{12} with a time-related dependency for the hydrophilic compounds. This is in contrast to findings from Viant et al. (2005), who found the variability of the metabolome more associated with the embryogenesis of a fish (medaka) than with exposure to trichloroethylene (Viant et al. 2005). Interestingly, after 14 h of exposure, the hydrophilic metabolite patterns of treatments draw back to the initial developmental stages of reference populations. This finding corresponds with results from the growth experiment (Fig. 1), where t_{14}-cells achieved a cell volume of about 75 fl after exposure, which was in the range of reference cells after 4 h of growth. These findings were not that clear in the lipophilic phase, where just t_{12}-cells showed a clear deviation from the controls. This may indicate that compensatory reactions of the cells to toxic exposure may be focussed on hydrophilic compounds. The PCA loading plot revealed which metabolites were responsible for the separation. Three different time-related response patterns of could be found, namely (i) an early exposure-specific increase in metabolites, (ii) late-observable effects on biosynthesis of metabolites and (iii) early exposure specific inhibition of biosynthesis of metabolites:

(i) During the first 4 h of exposure, an exposure-specific increase in biomolecules became evident in the 12-fold increase of Asp in comparison to t_0-cells (Table 1; Fig. 5a). An increase of metabolites might indicate a compensatory breakdown of proteins for energy supply or an accumulation of intermediate products. Asp is an essential metabolite in several anabolic processes, e.g. the pyrimidine synthesis. This pathway may be blocked, e.g. by insufficient supply with energy equivalents (ATP) from photosynthesis. After 4 h of exposure just small differences were found in the cell volume of exposed and reference algal populations (Fig. 1) indicating a high sensitivity of metabolite profiling to chemical exposure. Therefore, Asp might be used as a physiological marker in algal cells with early warning properties. Whether this substance meets the requirements for a biomarker could not be determined in this poof of principle study, but it illustrates the strategy for biomarker identification using this approach.

(ii) At later growth stages, inhibition of biosynthesis of additional metabolites became evident. The amino acids Lys and Gly increased in amount after 10 h of growth in healthy cells but not in exposed algal populations (Fig. 5) indicating long-term secondary effects of toxicants.

(iii) An early suppression of biosynthesis of carbohydrates was observed. Reduced energy supply from photosynthesis may provoke the cells to use catabolic pathways for energy supply. This became evident in the mobilisation of internal energy reserves like sugars. For example the rapid decrease

in mannose-6-phosphate in exposed algal populations during the first 4 h of exposure indicates the shortage of energy equivalents.

The metabolic pattern described above could clearly be explained from the mode-of-action (MoA) of the toxicant. Prometryn is specifically blocking the quinone site on the D1 protein of the PSII reaction centre within the thylakoid membrane. The PCA-pattern can be interpreted as a clear disturbance of the samples after 4 h of exposure followed by compensatory effects until 12 h and a return to initial cell stages after 14 h. Together with the underlying metabolite pattern, indicating a shortage of energy supply and a consumption of proteins and sugars for maintenance of vital cell functions, it may be seen as characteristic for the MoA of photosynthesis-inhibitors. The time-scaled pattern also gave insight into cascades of processes, related to primary and secondary toxic effects. To which extent this pattern varies in dependence on the MoA, remains future work. However, this proof of principle example may illustrate how stressor-specific metabolite pattern information may support MoA-analysis of unknown compounds.

5 Concluding remarks

From this proof of principle study several potential benefits from metabolomics for biomarker discovery and environmental risk assessment became evident: (i) Metabolites are often the first to react to stressors (Viant 2007). This became evident in the time-related patterns of metabolites detected in this study, as selected metabolites showed earlier responses in comparison to algal growth. (ii) The parallel analysis of algal growth parameters (cell volume) and metabolite composition indicates that metabolomics can support interpretation of well established toxicological assessment parameters. (iii) The study revealed multiple metabolic markers, responding to exposure, providing additional observation parameters to traditional endpoints in phytotoxicity assessment. (iv) Understanding toxicant-induced deviations from developmental metabolic trajectories may help to discriminate between primary and secondary toxic effects.

The conceptional framework to relate stress-induced metabolic responses to adverse biological outcomes, shown in this proof of principle study, indicates that metabolomics has a good potential to support environmental risk assessment of chemicals in future, even if genome information of a test species is not known. This makes metabolomics a promising future tool for ecotoxicology.

Acknowledgements We wish to acknowledge skilful support by Janet Krüger for technical assistance. We especially want to thank Mark Viant to initiate and edit this special issue. The financial support by the Commission of the European Community (MODELKEY, 511237-GOCE and KEYBIOEFFECTS, MRTN-CT-2006-035695) is gratefully acknowledged.

References

Adler, N. E., Schmitt-Jansen, M., & Altenburger, R. (2007). Flow cytometry as a tool to study phytotoxic modes of action. *Environmental Toxicology and Chemistry, 26*, 297–306. doi:10.1897/06-1636R.1.

Altenburger, R., Brack, W., Greco, W. R., Grote, M., Jung, K., Ovari, A., et al. (2006). On the mode of action of N-phenyl-2-naphthylamine in plants. *Environmental Science and Technology, 40*, 6163–6169. doi:10.1021/es060338e.

Altenburger, R., Callies, R., & Grimme, L. H. (1995). The mode of action of glufosinate in algae. *Pesticide Science, 45*, 305–310. doi:10.1002/ps.2780450403.

Altenburger, R., & Schmitt-Jansen, M. (2003). Assessments and predictions for ecosystems: Predicting toxic effects of contaminants in ecosystems using single species investigations. In A. M. Breure, B. A. Markert & H. G. Zechmeister (Eds.), *Bioindicators/biomonitors, principles, assessments, concepts* (pp. 153–198). Amsterdam: Elsevier Science.

Altenburger, R., Schmitt-Jansen, M., & Riedl, J. (2008). Bioassays with unicellular algae: Deviations from exponential growth and its implications for toxicity test results. *Journal of Environmental Quality, 37*, 16–21. doi:10.2134/jeq2006.0556.

Altenburger, R., Walter, H., & Grote, M. (2004). What contributes to the combined effect of a complex mixture? *Environmental Science and Technology, 38*, 6353–6362. doi:10.1021/es049528k.

Ankley, G. T., Daston, G. P., Degitz, S. J., Denslow, N. D., Hoke, R. A., Kennedy, S. W., et al. (2006). Toxicogenomics in regulatory ecotoxicology. *Environmental Science and Technology, 1*, 4055–4065.

Bölling, C., & Fiehn, O. (2005). Metabolite profiling of *Chlamydomonas reinhardtii* under nutrient deprivation. *Plant Physiology, 139*, 1995–2005. doi:10.1104/pp.105.071589.

Brack, W., Altenburger, R., Ensenbach, U., Möder, M., Segner, H., & Schüürmann, G. (1999). Bioassay-directed identification of organic toxicants in river sediment in the industrial region of Bitterfeld (Germany)—a contribution to hazard assessment. *Archives of Environmental Contamination and Toxicology, 37*, 164–174. doi:10.1007/s002449900502.

Broeckling, C. D., Huhman, D. V., Farag, M. A., Smith, J. T., May, G. D., Mendes, P., et al. (2005). Metabolic profiling of *Medicago truncatula* cell cultures reveals the effects of biotic and abiotic elicitors on metabolism. *Journal of Experimental Botany, 56*, 323–336. doi:10.1093/jxb/eri058.

Brown, M. R., & Jeffrey, S. W. (1992). Biochemical composition of microalgae from the green algal lasses Chlorophyceae and Prasinophyceae. 1. Amino acids, sugars and pigments. *Journal of Experimental Marine Biology and Ecology, 161*, 91–113. doi:10.1016/0022-0981(92)90192-D.

Bundy, J. G., Spurgeon, D. J., Svendsen, C., Hankard, P. K., Weeks, J. M., Osborn, D., et al. (2004). Environmental metabonomics: Applying combination biomarker analysis in earthworms at a metal contaminated site. *Ecotoxicology (London, England), 13*, 797–806. doi:10.1007/s10646-003-4477-1.

Cook, D., Fowler, S., Fiehn, O., & Thomashow, M. F. (2004). A prominent role for the CBF cold response pathway in configuring the low-temperature metabolome of *Arabidopsis*. *Proceedings of the National Academy of Sciences of the United States of America, 101*, 15243–15248. doi:10.1073/pnas.0406069101.

Dettmer, K., Aronov, P. A., & Hammock, B. D. (2007). Mass spectrometry-based metabolomics. *Mass Spectrometry Reviews, 26*, 51–78. doi:10.1002/mas.20108.

Ducruix, C., Vailhen, D., Werner, E., Fievet, J. B., Bourguignon, J., Tabet, J.-C., et al. (2008). Metabolomic investigation of the response of the model plant *Arabidopsis thaliana* to cadmium exposure: Evaluation of data pretreatment methods for further statistical analyses. *Chemometrics and Intelligent Laboratory Systems*, 67–77. doi:10.1016/j.chemolab.2007.08.002.

Ekman, D. R., Teng, Q., Jensen, K. M., Martinovic, D., Villeneuve, D. L., Ankley, G. T., et al. (2007). NMR analysis of male fathead minnow urinary metabolites: A potential approach for studying impacts of chemical exposures. *Aquatic Toxicology (Amsterdam, Netherlands), 85*, 104–112. doi:10.1016/j.aquatox.2007.08.005.

Escher, B. I., & Hermens, J. L. M. (2002). Modes of action in ecotoxicology: Their role in body burdens, species sensitivity, QSARs, and mixture effects. *Environmental Science and Technology, 36*, 4201–4217. doi:10.1021/es015848h.

Faust, M., Altenburger, R., Backhaus, T., Blanck, H., Boedeker, W., Gramatica, P., et al. (2001). Predicting the joint algal toxicity of multi-component s-triazine mixtures at low-effect concentrations of individual toxicants. *Aquatic Toxicology (Amsterdam, Netherlands), 56*, 13–32. doi:10.1016/S0166-445X(01)00187-4.

Faust, M., Altenburger, R., Bödeker, W., & Grimme, L. H. (1992). Algentoxizitätstests mit synchronisierten Kulturen. In K. G. Steinhäuser & P. D. Hansen (Eds.), *Biologische Testverfahren. Beiträge zu den Biotest-Statusseminaren 1989 und 1992* (pp. 311–321).

Fiehn, O., Kopka, J., Dörmann, P., Altmann, T., Trethewey, R. N., & Willmitzer, L. (2000). Metabolite profiling for plant functional genomics. *Nature Biotechnology, 18*, 1157–1161. doi:10.1038/81137.

Franz, S., Altenburger, R., Heilmeier, H., & Schmitt-Jansen, M. (2008). What contributes to the sensitivity of microalgae to triclosan? *Aquatic Toxicology (Amsterdam, Netherlands), 90*, 102–108. doi:10.1016/j.aquatox.2008.08.003

Guy, C., Kaplan, F., Kopka, J., Selbig, J., & Hincha, D. K. (2008). Metabolomics of temperature stress. *Physiologia Plantarum, 132*, 220–235.

Hansen, P.-D. (2008). Biosensors and ecotoxicology. *Engineering in Life Sciences, 8*, 26–31.

Hines, A., Oladiran, G. S., Bignell, J. P., Stentiford, G. D., & Viant, M. R. (2007). Direct sampling of organisms from the field and knowledge of their phenotype: Key recommendations for environmental metabolomics. *Environmental Science and Technology, 41*, 3375–3381. doi:10.1021/es062745w.

ISO 8692. (2002). *Water quality-fresh water algal growth inhibition test with unicellular green algae*. Geneva, Switzerland: International Organization for Standardization.

Jones, O. A. H., Spurgeon, D. J., Svendsen, C., & Griffin, J. (2008). Metabolomics based approach to assessing the toxicity of the polyaromatic hydrocarbon pyrene to the earthworm *Lumbricus rubellus*. *Chemosphere, 71*, 601–609. doi:10.1016/j.chemosphere.2007.08.056.

Kanazawa, T. (1964). Changes of amino acid composition of *Chlorella* cells during their life cycle. *Plant and Cell Physiology, 5*, 333–354.

Krupinska, K., & Humbeck, K. (1994). Light-induced synchronous cultures, an excellent tool to study the cell-cycle of unicellular green-algae. *Journal of Photochemistry and Photobiology B: Biology, 26*, 217–231. doi:10.1016/1011-1344(94)07069-5.

LeLay, P., Isaure, M.-P., Sarry, J.-E., Kuhn, L., Fayard, B., Le Bail, J.-L., et al. (2006). Metabolomic, proteomic and biophysical analyses of *Arabidopsis thaliana* cells exposed to a caesium stress. Influence of potassium supply. *Biochimie, 88*, 1533–1547. doi:10.1016/j.biochi.2006.03.013.

Lin, C. Y., Viant, M. R., & Tjeerdema, R. S. (2006). Metabolomics: Methodologies and applications in the environmental sciences. *Journal of Pesticide Science, 31*, 245–251. doi:10.1584/jpestics.31.245.

Moebus-Faust, S. (1994). Zur Analyse des intrazellulären, freien Aminosäure- und Polyaminpools in der einzelligen Grünalge *Chlorella fusca*. PhD-Thesis University of Bremen, Germany.

OECD guideline 201. (2006). *Freshwater alga and cyanobacteria growth inhibition test*. Paris: Organization for Economic Co-operation and Development.

Raimondo, S., Montague, B. J., & Barron, M. G. (2007). Determinants of variability in acute to chronic toxicity ratios for aquatic invertebrates and fish. *Environmental Toxicology and Chemistry, 26*, 2019–2023. doi:10.1897/07-069R.1.

Roessner, U., Wagner, C., Kopka, J., Trethewey, R. N., & Willmitzer, L. (2000). Simultaneous analysis of metabolites in potato tuber by gas chromatography-mass spectrometry. *The Plant Journal, 23*, 131–142. doi:10.1046/j.1365-313x.2000.00774.x.

Samuelsson, L. M., Forlin, L., Karlsson, G., Adolfsson-Erici, M., & Larsson, D. G. J. (2006). Using NMR metabolomics to identify responses of an environmental estrogen in blood plasma of fish. *Aquatic Toxicology (Amsterdam, Netherlands), 78*, 341–349. doi:10.1016/j.aquatox.2006.04.008.

Sarry, J.-E., Kuhn, L., Ducruix, C., Lafaye, A., Junot, C., Hugovieux, V., et al. (2006). The early responses of *Arabidopsis thaliana* cells to cadmium exposure explored by protein and metabolite profiling analyses. *Proteomics, 6*, 2180–2198. doi:10.1002/pmic.200500543.

Turner, M. A., Viant, M. R., Teh, S. J., & Johnson, M. L. (2007). Developmental rates, structural asymmetry, and metabolic fingerprints of steelhead trout (*Oncorhynchus mykiss*) eggs incubated at two temperatures. *Fish Physiology and Biochemistry, 33*, 59–72. doi:10.1007/s10695-006-9117-2.

Viant, M. R. (2007). Metabolomics of aquatic organisms: the new 'omics' on the block. *Marine Ecology Progress Series, 332*, 301–306. doi:10.3354/meps332301.

Viant, M. R., Bundy, J. G., Pincetich, C. A., de Ropp, J. S., & Tjeerdema, R. S. (2005). NMR-derived developmental metabolic trajectories: An approach for visualizing the toxic actions of trichloroethylene during embryogenesis. *Metabolomics, 1*, 149–158. doi:10.1007/s11306-005-4429-2.

Viant, M. R., Pincetich, C. A., Hinton, D. E., & Tjeerdema, R. S. (2006a). Toxic actions of dinoseb in medaka (*Oryzias latipes*) embryos as determined by in vivo 31P NMR, HPLC-UV and 1H NMR metabolomics. *Aquatic Toxicology (Amsterdam, Netherlands), 76*, 329–342. doi:10.1016/j.aquatox.2005.10.007.

Viant, M. R., Pincetich, C. A., & Tjeerdema, R. S. (2006b). Metabolic effects of dinoseb, diazinion and esfenvalerate in eyed eggs and alevins of Chinook salmon (*Oncorhynchus tshawytscha*) determined by 1H NMR metabolomics. *Aquatic Toxicology (Amsterdam, Netherlands), 77*, 359–371. doi:10.1016/j.aquatox.2006.01.009.

Viant, M. R., Walton, J. H., TenBrook, P. L., & Tjeerdema, R. S. (2002). Sublethal actions of cooper in abalone (*Haliotis rufescens*) as characterized by in vivo ^{31}P NMR. *Aquatic Toxicology (Amsterdam, Netherlands), 57*, 139–151. doi:10.1016/S0166-445X(01)00195-3.

Vitovà, M., & Zachleder, V. (2005). Points of commitment to reproductive events as a tool for analysis of the cell cycle in synchronous cultures of algae. *Folia Microbiol, 50*, 141–149. doi:10.1007/BF02931463.

Weckwerth, W., Wenzel, K., & Fiehn, O. (2004). Process for the integrated extraction, identification and quantification of metabolites, proteins and RNA to reveal their co-regulation in biochemical networks. *Proteomics, 4*, 78–83. doi:10.1002/pmic.200200500.